STYRELSEN FÖR

VINTERSJÖFARTSFORSKNING

WINTER NAVIGATION RESEARCH BOARD

Research Report No 128

Valtonen Ville

HULLFEM II - DIRECT CALCULATIONS METHODS FOR ICE STRENGTHENED HULLS, PART II

Finnish Transport and Communications Agency
Finnish Transport Infrastructure Agency
Finland

Swedish Maritime Administration
Swedish Transport Agency
Sweden

Talvimerenkulun tutkimusraportit — Winter Navigation Research Reports
ISSN 2342-4303
ISBN 978-952-311-905-5

FOREWORD

In this report no 128, the Winter Navigation Research Board presents the results of a research project HULLFEM II on direct calculations methods for ice strengthened hulls. The project continued work from HULLFEM I investigating plastic capacity of different ship hulls for the implementation of direct calculation methods for Finnish-Swedish Ice Class Rules.

The Winter Navigation Research Board warmly thanks Ville Valtonen for this report.

Helsinki

March 2024

Ville Häyrynen

Finnish Transport and Communications Agency

Amund Lindberg

Swedish Maritime Administration

Helena Orädd

Finnish Transport Infrastructure Agency

Fredrik Hellsberg

Swedish Transport Agency

Aker Arctic

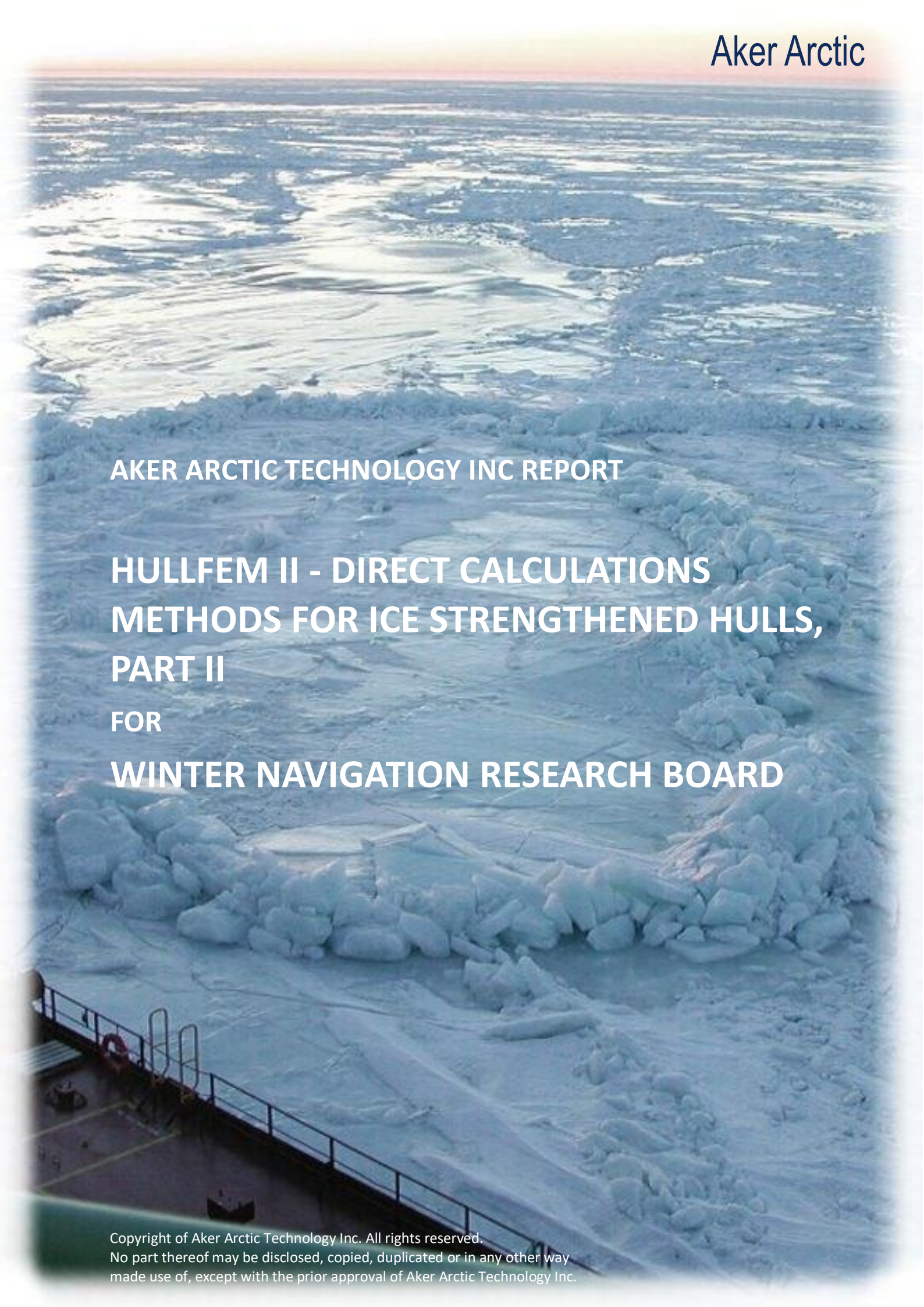

AKER ARCTIC TECHNOLOGY INC REPORT

HULLFEM II - DIRECT CALCULATIONS METHODS FOR ICE STRENGTHENED HULLS, PART II

FOR

WINTER NAVIGATION RESEARCH BOARD

Name of document: HULLFEM II - Direct calculations methods for ice strengthened hulls, part II			
Document Responsible: Ville Valtonen		**Document Co-Author(s):** Marko Ikkala (Meriflow) Vesa Niinilampi (Meriflow)	
Document Reviewer: Juuso Lindroos		**Document Approver:** Ville Valtonen	
Report number / Revision: K537 / B		**Status / Status Date:** Approved / 2023-12-29	
Client: Winter Navigation Research Board			
Revision remarks: First full version.			

Summary:

This study continues the work to form basis for direct calculation criteria for hull structures for vessels designed to Finnish-Swedish Ice Class Rules (FSICR). Methods originally developed in project HULLFEM were further refined. Wider and more varied set of vessels were analyzed, so that all relevant ship types, ship sizes and typical structural configurations relevant for the winter navigation on the Baltic Sea could be covered sufficiently. In addition, the vessels originally analyzed in the previous project were reanalyzed with the improved methods.

The results show that the plastic capacity of the ice strengthened structures follow the elastic capacity as defined in the FSICR, and is not dependent on ship size, ship type, ice class or structural configuration. Thus, it is possible to formulate design criteria that results in relatively similar scantlings as the current rules but is based on the plastic capacity. Based on the results of this study, the plastic capacity of shell plate is on average 277 % of elastic capacity. Plastic capacity of frames is on average 290 % of elastic capacity, and for primary structures 386 % of elastic capacity.

Keywords: Finnish-Swedish ice class rules (FSICR); Non-linear; Finite Element Method (FEM)			
Client reference: HULLFEM II		**Project number:** 30932	**Language:** English
Pages, total: 41	**Attachments:** 14 (323 pages)	**Distribution list:** Traficom, SMA, Väylä	**Confidentiality:** Copyright ©

TABLE OF CONTENTS

APPENDICES

1 INTRODUCTION

In the current Finnish-Swedish Ice Class Rules (FSICR) the direct calculation methods, such as finite element method (FEM) are not in general allowed for assessing the hull strength against ice loads. While the current prescriptive formulas have good service experience, they are somewhat limiting for the design. The goal of the HULLFEM II project is to continue the work of HULLFEM project to gather a better understanding of using direct calculation methods in the case of ice loads. This work aims to form a solid foundation for expanding the rules with provisions for direct analysis. The main aim of this continuation project is to study a wider array of ship types and structural configurations to broaden the applicability of the findings of HULLFEM.

Basic analysis methodology and modelling techniques were studied and established in 2022 in project HULLFEM. In HULLFEM, a sample of typical dry cargo vessels were analyzed with those methods.

The main content of this continuation study is to expand the applicability of the results from 2022 by analyzing additional ship types and structural arrangements to cover all typical vessels that operate on the Baltic Sea. In addition, the analysis methods from HULLFEM are refined with the learnings from the previous study to improve the accuracy of the results. Therefore, the dry cargo vessels from the previous study are reanalyzed in this study.

The goal is to form a sufficient knowledge basis for formulating the new rules / guidelines for use of direct calculations methods for the FSICR.

2 EXAMPLE VESSELS

2.1 SELECTING THE EXAMPLE VESSELS

The main aim of this study is to expand the applicability of the results of the previous study from general cargo vessels (see Figure 1 for example) to the various ship types operating on the Baltic Sea. To achieve this, some additional vessels were modeled. To ensure that all typical vessels are covered, Finnish Illustrated List of Ships from several years were studied.

2.1.1 GENERAL CARGO VESSEL

General cargo / dry cargo vessels are the most common vessel type on the Baltic Sea and were used as the example vessels in first part of the HULLFEM project [1]. These vessels typically have open cross-section, double hull and one or several holds for carrying diverse types of cargo either in bulk or as packaged goods. As the analysis methodology was developed based on the learnings of HULLFEM, these vessels are included in the analysis again.

Figure 1 Typical Baltic Sea general cargo vessel (photo Suomen kuvitettu laivaluettelo 2021).

2.1.2 ROPAX / PASSENGER FERRY

Typical RoPax / passenger ferry on Baltic Sea is about 200 to 220 m long and has ice class 1A super and relatively high engine power that allows high speed both in open water and ice. Typically, hull around icebelt includes mostly machinery spaces and tanks. Above that are first car decks and then accommodation. As these vessels carry a high number of passengers, typically from 2000 to 3000, the safety of these vessels is important and therefore it was considered important vessel type to be included in this study. Example of such vessel is shown in Figure 2.

Figure 2 Typical Baltic Sea RoPax ferry (photo Pjort Mahhonin / Wikipedia).

2.1.3 RORO VESSEL

Typical RoRo vessels are about equivalent size as the RoPax and have relatively similar structural arrangement on the hull, with mostly machinery spaces and tanks below the bulkhead deck. Above bulkhead deck, there is more car decks and less accommodation than on RoPax, and the car decks are higher to fit trucks. As the differences are mainly above bulkhead deck, they do not affect the ice strengthened region significantly. Ice class is typically either 1A or 1A super. Therefore, it was considered that the results of the RoPax are applicable to typical RoRo vessels. Examples of such vessels are shown in Figure 3.

Figure 3 Typical RoRo vessels on Baltic Sea (photos Finnlines).

2.1.4 TANKER, LIQUID CARGO

Tankers for oil and other liquid cargos have relatively similar side structure as the general cargo vessels analyzed in the previous study. However, possibly important difference is that tankers have a solid main deck, opposed to open-top hull of general cargo vessels. In

addition, any accident involving an oil tanker has a risk of an environmental catastrophe, and thus it was considered important to include a typical large tanker into this study. In Baltic Sea context, the largest typical tankers are Aframax size. These large tankers typically carry crude oil. Example of a large tanker is shown in Figure 4.

Figure 4 Typical large tanker on Baltic Sea (photo Neste).

In addition, there are several smaller sizes of tankers trading on the Baltic Sea, most carrying either chemicals or oil products. These can be combined with the LNG tanker discussed in the next chapter, as the structure of the ice-reinforced side is similar, and the main cross section is also relatively similar. Example of a smaller tanker is shown in Figure 5.

Figure 5 Typical small chemical / product tanker on Baltic Sea (photo Wikimedia commons).

2.1.5 TANKER, GAS

Tankers for gas (typically LNG) have three main configurations, either with membrane tank, bilobe tanks or spherical tanks. For purposes of this study, vessels with membrane tanks have similar structural principles as tankers for liquid cargos. Vessels with bilobe tanks have relatively similar structures, with the main deck typically somewhat higher than in liquid tankers due to the lower density of the cargo. Spherical tank vessels are open-top configuration, with similar principle as general cargo vessels in chapter 2.1.1, and are sufficiently covered by those. For a smaller tanker, it is chosen to study a bilobe-type LNG tanker. The results of that cover sufficiently the smaller liquid tankers and membrane-type LNG tankers. Typical Baltic Sea LNG tanker is shown in Figure 6.

Figure 6 Typical Baltic Sea LNG carrier (photo Gasum).

2.1.6 BULK CARRIER

Bulk carriers have typically structure and cross section that falls between general cargo vessels and tankers. Otherwise, bulk carriers would be sufficiently covered by analyzing these, but as the question about single side structures arose in the previous study [1], the medium-sized general cargo vessel was modified to a single side configuration. The most practical way for that was to convert it to a bulk carrier. Example of a typical bulk carrier is shown in Figure 7.

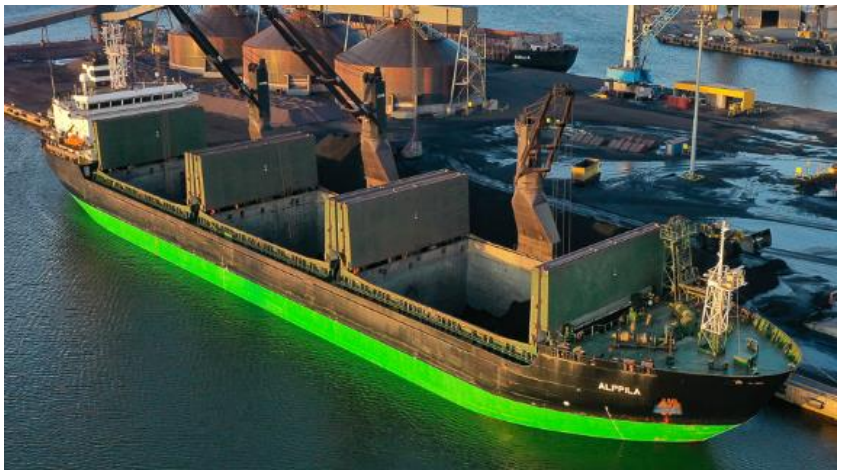

Figure 7 Typical Baltic Sea bulk carrier (photo ESL shipping).

2.1.7 CONTAINER VESSEL

While there are differences in hatches, transverse bulkheads & such, the side structure of the container vessels is similar to the general cargo vessel, and it is considered to be covered by that. Example of a typical Baltic Sea container vessel is shown in Figure 8.

Figure 8 Typical Baltic Sea container vessel (photo J & H. Soinila / Suomen kuvitettu laivaluettelo 2021).

2.1.8 SMALL SHIPS

While the Finnish-Swedish Ice Class Rules are also used in design of small archipelago ferries, tugboats & such, examples shown in Figure 9 and Figure 10, the rules are not aimed for these. Therefore the applicability of the new guidelines is not studied on those vessel types. It is also recognized that most of these vessels are likely to be in any case be designed with the prescriptive rule formulas in the foreseeable future.

Figure 9 Typical archipelago ferry (photo Sofia Ek / Wikimedia commons).

Figure 10 Typical tug (photo Alfons Håkans).

2.2 DESIGN OF THE EXAMPLE VESSELS

Similar to the previous study, the main dimensions of the example vessels were chosen based on available reference designs and using methods from [2]. Scantlings have been calculated with DNV Nauticus to fulfill basic classification, and in general chosen to be reasonable and typical for the vessel type in question, to represent a typical design as closely as possible.

For ice class, scantlings were chosen to be lowest possible that fulfill the requirements of the current FSICR [3], as explained in more detail in the following chapter.

All example vessels were designed using HT-36 grade steel, as that is a relatively typical material in current shipbuilding.

2.3 REANALYSIS OF VESSELS FROM HULLFEM

Based on the previous study, some changes were made to the baseline vessel to improve the accuracy of the results, and the analysis was rerun for these.

Typically, the scantlings of a ship are chosen from available standard materials in such way that plate thicknesses are rounded to closest full (or half) millimeter. Similarly, the frame profiles are chosen from list of standard profiles as the smallest standard size that fulfills shear area and section modulus requirements. Due to this, there is in most cases some margin, as it is rare that the available thicknesses and profiles would be exact match for the rule requirement.

However, for finding the exact plastic capacity that the minimum structure compliant with the current rules has, this variation should be removed. Thus, all vessels from previous study were modified to have shell plate thickness that is exactly the rule required with accuracy of 0.1 mm. As the rules specify required net thickness and a corrosion margin to account for wear and corrosion, the calculation was done with the net thickness, i.e. the corrosion addition was deducted from the shell plate thickness. For internal members, corrosion deduction was not made, as that is not done in the current rules. [3]

For profiles, custom profiles with minimum allowable properties were used. As bulb profiles are typically used on ships that are covered by the FSICR, these were used. Profile thicknesses were chosen to fall within the range typical to the height of the profile, and to fulfill the requirements of the FSICR. The profile height was varied to find the minimum that fulfills the FSICR requirements for shear area and section modulus.

One main finding of the previous study was that for the typical double side structure, minimum thickness requirement results in webframes and stringer platforms to have significant extra capacity over the minimum requirements of ice class rules. To assess how the proposed new criteria would relate to structure fulfilling the current FSICR, the general cargo vessels with double side were modified to bulk carriers with single side with open T-beam webframes and stringers, even though that is less typical structural arrangement nowadays.

2.4 SMALL DRY CARGO VESSEL

This vessel was analyzed in the previous study and is now reanalyzed with modifications in scantlings explained in 2.3. This vessel has transverse framing with intermediate frames spaced at 400 mm. The main dimensions are shown in Table 1 and the midship section in Appendix A. This vessel is of similar type as shown in Figure 1 and described in chapter 2.1.1, and represents the smaller end of ice strengthened fleet on the Baltic Sea.

Table 1 Main dimensions of small dry cargo vessel.

FSICR	**1A**		*Ice class*
L_{oa}	84.0	m	*Length, overall*
L_{bp}	78.8	m	*Length, rule*
B	14.0	m	*Breadth*
D	7.0	m	*Depth*
T	5.7	m	*Draught*
Δ	4960	t	*Displacement*
C_b	0.77		*Block coefficient*
v	12	kn	*Service speed*
P	1650	kW	*Shaft power*

2.5 MEDIUM DRY CARGO VESSEL

This vessel was analyzed in the previous study and is now reanalyzed with modifications in scantlings explained in 2.3. This vessel was analyzed for three different ice classes, 1C, 1A and 1A super. The 1C vessel has longitudinal framing with spacing of 600 mm, while 1A and 1A super have transverse framing with intermediate frames spaced at 400 mm, representing typical configurations for each ice class. The main dimensions for each variant are shown in Table 2 and the midship sections in Appendix A. This vessel is similar type as shown in Figure 1 and described in chapter 2.1.1, and of most typical size on the Baltic Sea [1]. As discussed in chapter 2.1.7, this also covers typical container vessels, due to similar structure around ice strengthened part of the hull.

Table 2 Main dimensions of medium dry cargo vessels.

FSICR	**1A**	**1C**	**1A super**		*Ice class*
L_{oa}	121	120.2	122.6	m	*Length, overall*
L_{bp}	115	115	115	m	*Length, rule*
B	20.3	20.3	20.3	m	*Breadth*
D	10.7	10.7	10.7	m	*Depth*
T	7.4	7.4	7.4	m	*Draught*
Δ	14200	14100	14360	t	*Displacement*
C_b	0.80	0.80	0.81		*Block coefficient*
v	12	12	12	kn	*Service speed*
P	4000	3000	5500	kW	*Shaft power*

2.6 LARGE DRY CARGO VESSEL

This vessel was analyzed in the previous study and is now reanalyzed with modification explained in 2.3. This vessel has longitudinal framing with spacing of 700 mm. The main dimensions are shown in Table 3 and the midship section in Appendix A. This vessel is of similar type as shown in Figure 1 and described in chapter 2.1.1, and of about the typical maximum size used in the Baltic Sea.

Table 3 Main dimensions of large dry cargo vessel.

FSICR	**1A**		*Ice class*
L_{oa}	196	m	*Length, overall*
L_{bp}	184	m	*Length, rule*
B	32.26	m	*Breadth*
D	18.6	m	*Depth*
T	13.0	m	*Draught*
Δ	69930	t	*Displacement*
C_b	0.88		*Block coefficient*
v	12	kn	*Service speed*
P	14750	kW	*Shaft power*

2.7 MEDIUM BULK CARRIER

This vessel is similar to medium dry cargo vessel analyzed in the previous study, except that the side has been changed from double skin to single skin construction. As single skin construction is not practical for a typical dry cargo vessel, a bulk carrier was chosen instead. Main dimensions are identical, meaning that although the vessels are nominally of different ship type, in practice this is a direct comparison between two structural arrangements.

To assess the effect of varying structural configurations, this vessel is analyzed with several structural configurations (frame spacings include intermediate frames, if present):

- transverse framing with intermediate frames spaced at 400 mm (same as original dry cargo vessel)
- transverse framing with spacing of 600 mm
- transverse framing with spacing of 800 mm
- longitudinal framing with spacing of 400 mm
- longitudinal framing with spacing of 600 mm

The main dimensions are shown in Table 4 and the midship sections in Appendix A. This vessel type is described in chapter 2.1.6 and typical example is shown in Figure 7.

Table 4 Main dimensions of medium bulk carrier.

FSICR	1A		*Ice class*
L_{oa}	121	m	*Length, overall*
L_{bp}	115	m	*Length, rule*
B	20.3	m	*Breadth*
D	10.7	m	*Depth*
T	7.4	m	*Draught*
Δ	14200	t	*Displacement*
C_b	0.80		*Block coefficient*
v	12	kn	*Service speed*
P	4000	kW	*Shaft power*

2.8 ROPAX

The RoPax vessel was designed to represent a typical ferry on for example routes Helsinki – Tallinn and Turku – Stockholm and similar. This vessel has single side configuration. The model is made up to strength deck, and the deckhouse above that is not considered to be structurally effective. The main dimensions for the RoPax vessel are shown in Table 5 and the midship section in Appendix A. As discussed in chapter 2.1.3, this vessel covers RoPax vessels and passenger ferries discussed in chapter 2.1.2 and RoRo vessels discussed in chapter 2.1.3 as both have relatively similar structure on the ice-strengthened hull. Typical example of a Baltic Sea RoPax ferry is shown in Figure 2.

Table 5 Main dimensions of RoPax ferry.

FSICR	1A super		*Ice class*
L_{oa}	218.5	m	*Length, overall*
L_{bp}	200	m	*Length, rule*
B	31.8	m	*Breadth*
D	9.8	m	*Depth*
T	7.0	m	*Draught*
Δ	31605	t	*Displacement*
C_b	0.69		*Block coefficient*
v	22	kn	*Service speed*
P	10500	kW	*Shaft power*

2.9 MEDIUM LNG TANKER

Small / medium LNG tanker was chosen to be of relatively same size as the dry cargo / bulk carriers, to assess if the addition of full main deck has an effect on the plastic capacity of the ice belt. It is called medium in this report for consistency with other vessels, even though as a tanker it could be well considered to be small. The vessel is designed to have bilobe tanks, as that is relatively common choice for that size. The main dimensions are shown in Table 6 and the midship section in Appendix A. This vessel

covers smaller end of oil tankers discussed in chapter 2.1.4 and gas tankers discussed in 2.1.5. Example of a typical small / medium sized LNG tanker is shown in Figure 6.

Table 6 Main dimensions of medium LNG tanker.

FSICR	**1A**		*Ice class*
L_{oa}	105	m	*Length, overall*
L_{bp}	102.3	m	*Length, rule*
B	17.8	m	*Breadth*
D	10.9	m	*Depth*
T	7.0	m	*Draught*
Δ	9400	t	*Displacement*
C_b	0.72		*Block coefficient*
v	12	kn	*Service speed*
P	3900	kW	*Shaft power*

2.10 LARGE OIL TANKER

Large tanker was designed to represent typical largest crude oil tankers that operate on the Baltic Sea. These are Aframax-size tankers. As oil tankers are mandated to have double side, this vessel was designed with a double side structure. The main dimensions are shown in Table 7 and the midship section in Appendix A. This vessel covers larger end (in Baltic Sea context) of oil tankers discussed in chapter 2.1.4 and gas tankers discussed in 2.1.5. Example of a typical large tanker is shown in Figure 4.

Table 7 Main dimensions of large oil tanker.

FSICR	**1A**		*Ice class*
L_{oa}	250	m	*Length, overall*
L_{bp}	240	m	*Length, rule*
B	44	m	*Breadth*
D	22	m	*Depth*
T	15.25	m	*Draught*
Δ	132500	t	*Displacement*
C_b	0.80		*Block coefficient*
v	14	kn	*Service speed*
P	15700	kW	*Shaft power*

3 METHODS

The methodology follows principles established in the first part of the HULLFEM project [1]. For more detailed information and background for choosing these methods, the reader is referred to that report. For clarity, the used methods are summarized here. The changes and improvements made to the methods used in the previous work are presented in more detail here.

3.1 FINITE ELEMENT MODEL

3.1.1 MODELING

The vessels were modeled and meshed in NAPA Designer. The mesh was then exported to Abaqus/CAE. Loads, boundary conditions, etc. were applied in Abaqus/CAE. The model was analyzed using Abaqus/Standard, and postprocessed in Abaqus/Viewer.

Model extents were taken as half ship, i.e. from centerline to side shell on one side, from baseline to strength deck, and six webframe spacings. Six webframe spacings was chosen because that provides at minimum two webframe spacings between the load and the boundary condition, preventing boundary effects from affecting the results with the dimensions of the example vessels. This model size was found to be the smallest suitable, based on earlier study [1].

3.1.2 MESHING

Models were made fully with linear shell elements. Bulb profiles were modeled as equivalent L-profiles. In Abaqus documentation, element types S4R and S3R, which are quadrilateral (4-node) and triangular (3-node) general- purpose shell elements with reduced integration, hourglass control, and finite strain, are recommended for this type of analysis and these element types were used in this study [4].

As the model is made with shell element, the bulb profiles were converted to equivalent L-profiles. Like previous study, this was done based on the CSR formula [1]. However, the shell element thickness is by default distributed evenly on both sides of the moulded surface. This results in lower effective height for the stiffener, reducing the section modulus significantly. Modifying the thickness offset for each frame and girder in correct way would be very time-consuming and error-prone handwork, and therefore alternative method was developed.

As illustrated in Figure 11, the web height of the equivalent L-profile was increased by half of plate thickness of equivalent flange and shell plate. While this introduces minor error in shear capacity of the frame profile, and very minor error in section modulus due to excess web height, testing proved that this idealization offers much more exact representation of the actual bending capacity of the frame, and thus was taken into use.

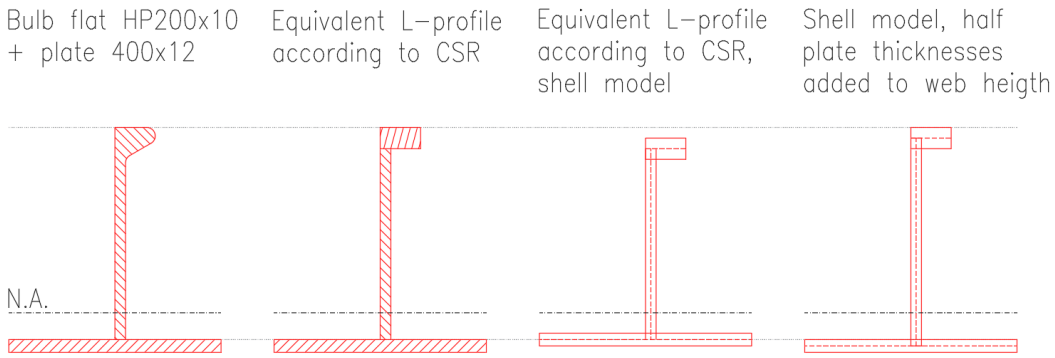

Figure 11 Idealization of bulb flat as L-profile. For clarity, effective plate width is halved in figure.

Mesh density was taken as minimum 8 elements on shell plate between each stiffener, and as minimum 3, preferably 4, elements across stiffener web. These mesh density guidelines follow the recommendations of Classification Societies for similar type of analysis [5] [6] [7], and were found to work well on the first part of the HULLFEM project [1].

3.1.3 MATERIAL MODEL

Material was modeled as bilinear elastic-plastic with plastic modulus E_t of 1000 MPa, as this model is widely used, see for example [5], [6] and [8], and in the previous study [1], it was found to produce very similar results to more complicated material models found in [6] and [7] at the relevant deformations [1]. As per Abaqus convention, all stresses and strains are taken as true stress and true strain. The material parameters for HT-36 grade steel are shown in Table 8.

Table 8 Material parameters for HT-36 steel.

Steel grade	Yield	Ultimate		Elongation	Abaqus material model			
					Yield		Ultimate	
		min	max	A_{50}	σ	ε_{pl}	σ	ε_{pl}
HT-36	355	490	620	21 %	355.6	0.0	681.6	0.1873

3.1.4 LOAD

Load is applied as rectangular patch with evenly distributed pressure, similar to the previous study [1]. The load patch dimensions are taken directly from the Finnish-Swedish Ice Class Rules [3], as that was found to be reasonable approach in the previous study [1]. The load patch lengths for various structural elements are shown in Table 9.

Table 9 Load patch lengths for various structures [3].

Structure	Type of framing	l_a [m]
Shell	Transverse	Frame spacing
	Longitudinal	1.7×Frame spacing
Frames	Transverse	Frame spacing
	Longitudinal	Span of frame
Ice Stringer		Span of stringer
Web frame		2×Web frame spacing

The load is applied to elements as pressure load. The element mesh does not always align perfectly with the load patches. The applied load patch area was taken always as the closest possible match to load patch dimensions from the rules. Then, the pressure was adjusted to obtain equivalent force:

$$p_{FEM} = p_{Rules} \frac{A_{Rules}}{A_{FEM}}$$

Exact load areas, locations, patch sizes and pressures for each vessel and load case are shown in Appendixes B to N. The error in load patch dimensions is less than half of element size, which varies between 40 and 80 mm depending on the ship type, meaning that the error in each load patch dimension varies between 20 and 40 mm. Compared to typical load patch height of 220 to 350 mm and width of 400 to 4800 mm, the error can be considered small. Example of load application is shown in Table 10.

Table 10 Load patch locations, dimensions, and load for medium bulk carrier with transverse framing at 400 mm spacing.

	Location		Rules					Model	
	X	Z	p	l	h	A	F	A	p
	mm	mm	MPa	mm	mm	cm2	kN	cm2	MPa
Shell	6200	5800	1.306	400	300	1200	157	1280	1.224
Frame	6000	5700	1.306	400	300	1200	157	1120	1.399
Stringer	6000	6800	0.653	2400	300	7200	470	7680	0.612
Webframe 1	7200	7400	0.462	4800	300	14400	665	15360	0.433
Webframe 2	7200	6800	0.462	4800	300	14400	665	15360	0.433
Webframe 3	7200	5800	0.462	4800	300	14400	665	15360	0.433
Webframe 4	7200	4800	0.462	4800	300	14400	665	15360	0.433

In this study, load was applied to find the plastic capacities as defined in 3.2.3 for shell plate, frame, stringer (for transversally framed vessels) and web frames. In addition, shell analysis was run up to permanent deformation of 5 % of frame spacing, as that was found in the previous study to be the upper limit of ice related damages on the Baltic Sea [1], and can be therefore thought to be the absolute maximum for the load that the structure must be able to withstand without major failure.

On analyzing the results, shell, frames, and primary structures were analyzed separately. Stringers and web frames were combined as the primary structures, as these are on the same level on the structural hierarchy, have similar factor of safety on the current FSICR (f_7 for stringers and f_{12} for web frames are both set at 1.8 [3]), and as the failure modes between these were linked. In several cases, load applied on stringer caused first failure on web frame, and vice versa, making it most sensible to assess these together.

For each structural member, most onerous location(s) for the load patch were selected, following the findings from the previous study [1]. In case the most onerous location was not obvious, several locations were used to find the most onerous one. Example of typical load patch locations is shown in Figure 12. Similar logic was followed for each vessel. All load patch locations and exact load patch dimensions, pressures, etc. are shown in Appendixes B to N.

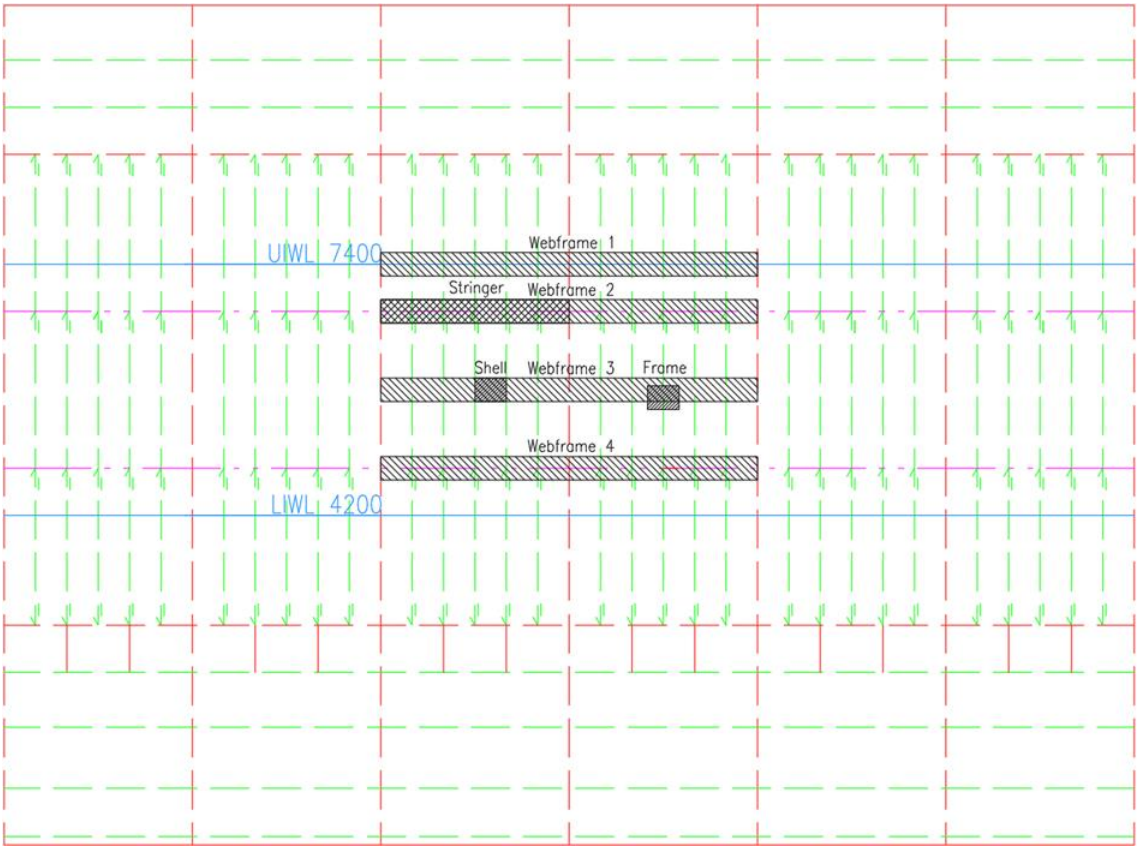

Figure 12 Load patch locations for bulk carrier with transverse framing at 400 mm spacing.

3.1.5 BOUNDARY CONDITIONS

Boundary conditions were applied using the practices that were found to work well on the previous study [1]. Boundary conditions were applied to the model edges where the structure continues. At centerline, Y-symmetry boundary condition was applied. At model ends, pinned boundary condition was applied.

In case there were additional structure, such as deckhouse, above strength deck, it was considered not effective for carrying ice loads, and therefore omitted and not modeled as boundary condition.

Example of loading and boundary conditions is shown in Figure 13. Boundary condition marked in orange at the ends refers to pinned boundary, and boundary condition marked at centerline with blue and orange refers to y-symmetry. Applied pressure load is shown in magenta.

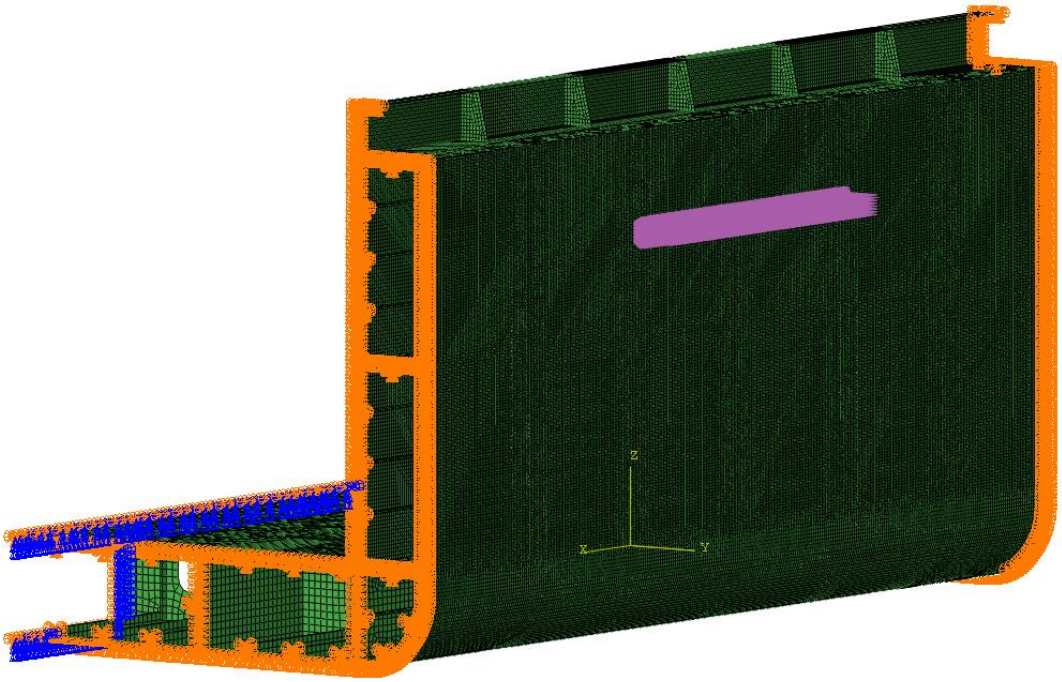

Figure 13 Typical boundary conditions and load patch on model of small general cargo vessel.

3.2 ANALYSIS

3.2.1 SOLUTION AND INCREMENTATION

The analysis is made with implicit solver.

Incrementation is set automatic, so that Abaqus solver can vary the load increment to find optimum for obtaining a stable solution with minimum computational effort. Selecting suitable maximum load increment is a balance between acceptable accuracy and computational cost. To find the most appropriate maximum load increment, several options were tested.

For cases where the response was governed by plastic hinge type mechanisms or very gradual buckling, it was found that Abaqus automatic incrementation works as intended and provides accurate results. For these cases, the result did not change if smaller increments were used. Thus, automatic incrementation was used for all cases where the iteration converged easily, and no special reason was found for further investigation.

The step size for the automatic incrementation varies with the load. For some of the more complicated cases, where the response is governed by a rapid buckling failure, it was found that this variation in increment affected the results. Thus, for these cases, it was found necessary to control the maximum step size, to ensure that onset of rapid buckling was captured accurately by incrementing the load with sufficiently small steps. The maximum load increment values shown in Table 11 were found to offer reasonable balance between accuracy and computational cost for these problems and were used when found necessary. In all cases, Abaqus Solver was allowed to use smaller load increments when necessary to find a stable and accurate solution.

Table 11 Maximum load increments for the solver, as percentage of total load.

Load	Maximum increment
0 % - 60 %	0.1
60 % - 75 %	0.02
75 % - 85 %	0.01
85 % - 92.5 %	0.005
92.5 % - 100 %	0.0025

3.2.2 ITERATION

In the previous project, HULLFEM, the permanent deformation was obtained by subtracting the elastic deformation from the total deformation [1]. This method is relatively straightforward to apply and provides reasonably accurate results for structures that fail in bending via plastic hinge mechanisms. However, in case of deformation that is governed by buckling, the underlying assumptions behind that method that the elastic deformation is proportional to the loading, is generally not valid. Therefore, to improve the accuracy of the calculation, alternative method would be needed.

When calculating the permanent deformation of the structure after being subjected to a known load, the permanent deformation can be obtained directly, by first loading and then unloading the structure in FE. This is the method recommended when analyzing a structure according to the proposed new rules.

However, for calculating the capacity of a known structure at a known deformation, the calculation cannot be performed directly. Instead, initial guess of the load is made, the deformation is calculated, and then the load is adjusted iteratively to find the load corresponding to the target deformation. In practice, this was achieved by programming a python script that ran Abaqus analysis iteratively until the load to cause the desired permanent deformation was found.

In most cases, the iteration converged well, and it was possible to find the load corresponding to the exact desired deformation. However, in couple of cases, the buckling was very rapid, and deformation increased very rapidly after the limit load was reached. In those cases, slight deviation on the final permanent deformation was accepted, as long as the error on the load was small (less than 1 % of the rule load).

In case 1000 % of the FSICR design ice load did not result in a permanent deformation exceeding the limits discussed in chapter 3.2.3, iteration was not continued, and 1000 % was shown as the result for that particular load case. For small dry cargo vessel, 900 % was used due to convergence issues. In practice, both of these mean that the design of that particular structural member is not driven by ice class requirements. For all vessels and each structural member, there was at least one load case that resulted in lower load than these limits.

3.2.3 DEFINITION OF CAPACITY LIMIT

The plastic capacity of the structure is defined as the load at which the permanent deformation of the structure exceeds the limits of IACS newbuilding quality standard [9]. For the structures in question, this limit is most typically 8 mm or 0.3 % of span for framing members. As discussed in the previous study [1], the limit is taken as follows:

- 8 mm for shell plate
- 0.3 % of span for all framing members, but in no case less than 8 mm
- 8 mm for out-of-plane deformation of all members

In addition, it is required that stresses stay below specified minimum ultimate strength of the material. For the HT-36 grade steel used, that limit is 490 MPa in engineering stress, and 557.0 MPa in true stress used by Abaqus.

4 RESULTS

In this chapter, the main results are presented. More detailed results, load-displacement curves as well as stress and displacement plots are presented in Appendixes B to N.

4.1 SMALL DRY CARGO VESSEL

The load at which each structural element will reach the permanent deformation limits defined in 3.2.3 are shown in Table 12.

For shell plate and frames, the model behaves in expected way and plastic behavior follows classical plastic hinge mechanism. No instability was observed in framing.

For stringer, it was not possible to determine the limit, as the failure happened by very rapid buckling which caused convergence errors, but at 900 % of the rule design load, the permanent deformation was 0.2 mm, and it can be clearly concluded that all other structural elements will fail before the stringer in this case. Thus, for this vessel, stringer platform design is clearly driven by other considerations than ice load, and the resulting stringer platform has ample capacity for ice loads.

For web frames, the limiting load case was webframe 1, with out-of-plane deformation of main deck as the limiting factor. In all cases, out-of-plane deformation, in practice buckling, was the limiting factor, which is typical to plate webframes in double side.

Table 12 Loads (as percentage of rule design load) to cause the structural member to reach permanent deformation limit as defined in 3.2.3 for the small dry cargo vessel.

Load case	Load
Shell	286.8 %
Frame	296.6 %
Primaries	473.3 %
Shell 5%	398.8 %

4.2 MEDIUM DRY CARGO VESSEL, IC

The load at which each structural element will reach the permanent deformation limits defined in 3.2.3 are shown in Table 13.

For shell plate and frames, the model behaves in expected way and plastic behavior follows classical plastic hinge mechanism. No instability was observed in framing. It is noted that plastic capacity of the shell plate exceeds that of the frames, while proper hierarchy would require frames to be as strong or stronger than shell plate.

Web frames and platforms were loaded up to 1000 % of the rule load, and except for load case webframe 6, permanent deformation remained below limit of 8 mm for all cases. For webframe 6, the limiting factor was out-of-plane deformation on webframe, i.e. buckling. For this vessel, webframe and platform design is clearly driven by other considerations than ice load, and the primary structures have ample capacity for ice loads.

Table 13 Loads (as percentage of rule design load) to cause the structural member to reach permanent deformation limit as defined in 3.2.3 for the medium dry cargo vessel with ice class IC.

Load case	Load
Shell	362.5 %
Frame	293.3 %
Primaries	832.4 %
Shell 5%	732.2 %

4.3 MEDIUM DRY CARGO VESSEL, IA

The load at which each structural element will reach the permanent deformation limits defined in 3.2.3 are shown in Table 14.

For shell plate and frames, the model behaves in expected way and plastic behavior follows classical plastic hinge mechanism. No instability was observed in framing.

Stringer platform was loaded up to 1000 % of rule load, and permanent deformation remained below limit of 8 mm. It can be clearly concluded that all other structural elements will fail before the stringer platform in this case. Thus, for this vessel, stringer platform design is clearly driven by other considerations than ice load, and the stringer platform that has ample capacity for ice loads.

For load patches on web frames, the limiting load case was webframe 5, with out-of-plane deformation of lowest stringer platform as the limiting factor. In load cases webframe 1 and 3, 1000 % of rule load was reached before the permanent deformation limit of 8 mm, and these are clearly not the dimensioning ones for the webframe. In all other cases, out-of-plane deformation, in practice buckling, was the limiting factor, which is typical to plate webframes in double side.

Table 14 Loads (as percentage of rule design load) to cause the structural member to reach permanent deformation limit as defined in 3.2.3 for the medium dry cargo vessel with ice class IA.

Load case	Load
Shell	290.6 %
Frame	276.8 %
Primaries	348.9 %
Shell 5%	453.8 %

4.4 MEDIUM DRY CARGO VESSEL, IASUPER

The load at which each structural element will reach the permanent deformation limits defined in 3.2.3 are shown in Table 15.

For shell plate and frames, the model behaves in expected way and plastic behavior follows classical plastic hinge mechanism. No instability was observed in framing.

The same stringer platform that was able to withstand 1000 % of the rule ice load for ice classes IC and IA will fail by buckling at 745 % of IAsuper ice load. While it still is the last element of the structure to fail, and all other structures reach failure criteria at lower load, this shows that different aspects of the hull structure might become relevant at higher ice loads. Still, it is clear that the design of the platform is driven by other requirements than ice loads, and as result of those, it has ample capacity for ice.

For load on web frames, the capacity is limited by buckling of the stringer platform. Mainly this seems to be governed by the bending capacity of the platform stiffener. As typical for relatively well stiffened plate structures in double side, these have ample capacity for the ice load, and it is probable that the design of webframes is not driven by ice loads for this vessel. It is noted that due to slightly different arrangement of manholes and stiffeners than for IA variant, the buckling capacity of the web frame is increased significantly and is not the limiting factor for this vessel.

Table 15 Loads (as percentage of rule design load) to cause the structural member to reach permanent deformation limit as defined in 3.2.3 for the medium dry cargo vessel with ice class IAsuper.

Load case	Load
Shell	276.4 %
Frame	321.3 %
Primaries	568.0 %
Shell 5%	414.1 %

4.5 LARGE DRY CARGO VESSEL

The load at which each structural element will reach the permanent deformation limits defined in 3.2.3 are shown in Table 16.

For shell plate and frames, the model behaves in expected way and plastic behavior follows classical plastic hinge mechanism. No instability was observed in framing.

For web frames, the limiting factor is buckling of the webframe. This is typical behavior for plate-type webframes in double side construction.

Table 16 Loads (as percentage of rule design load) to cause the structural member to reach permanent deformation limit as defined in 3.2.3 for the large dry cargo vessel.

Load case	Load
Shell	310.8 %
Frame	310.0 %
Primaries	439.3 %
Shell 5%	556.5 %

4.6 MEDIUM LNG TANKER

The load at which each structural element will reach the permanent deformation limits defined in 3.2.3 are shown in Table 17.

For shell plate and frames, the model behaves in expected way and plastic behavior follows classical plastic hinge mechanism. No instability was observed in framing.

For stringer, the model follows classical plastic hinge mechanism. No instability (web buckling or tripping) was observed in the stringer profile before reaching the permanent deformation limit in perpendicular to shell direction.

For web frames, the behavior was governed by web buckling. This is due to relatively large, unstiffened plate field of the web. Typically, the nature of this type of buckling is relatively sudden, leading to rapid loss of load-carrying capacity after buckling onset. This structure is according to current rules, and this sort of failures have been observed on damaged vessels [10]. Based on these observations, it is recommended that some sort of buckling prevention requirement would be considered for the rules. Obviously, non-linear finite element analysis is one solution, but as it is likely that prescriptive rules will also be continued to be used due to significantly smaller effort needed, prescriptive guidance for buckling stiffeners would be useful.

For load case web frame 1, it was not possible to iterate exact load at which the permanent deformation is exactly at the limit specified in 3.2.3, due to very rapid buckling of the webframe. However, as the permanent deformation limit was not reached at 429.0 % of the rule load and was significantly exceeded at 429.1 % of the rule load, it can be concluded that with sufficient accuracy the capacity is 429.0 %. For all other load cases, the iteration converged successfully.

Table 17 Loads (as percentage of rule design load) to cause the structural member to reach permanent deformation limit as defined in 3.2.3 for the medium LNG tanker.

Load case	Load
Shell	269.9 %
Frame	265.7 %
Primaries	350.2 %
Shell 5%	403.0 %

4.7 LARGE TANKER

The load at which each structural element will reach the permanent deformation limits defined in 3.2.3 are shown in Table 18.

For shell plate and frames, the model behaves in expected way and plastic behavior follows classical plastic hinge mechanism. No instability was observed in framing.

For webframes, the limiting factor is buckling. This is typical to double side construction. For this vessel, the limiting factor for buckling capacity is the longitudinally stiffened platforms, which are very typical for this type of vessel, as the longitudinal stiffening is

needed to resist buckling from global hull girder loads. As is typical for tankers (and bulk carriers), the dimensions of the platforms and web frames are mainly driven by the Common Structural Rules, and less by the FSICR. Still, the resulting structure and it's capacity aligns reasonably well with other ice strengthened vessels.

Table 18 Loads (as percentage of rule design load) to cause the structural member to reach permanent deformation limit as defined in 3.2.3 for the large tanker.

Load case	Load
Shell	289.6 %
Frame	287.1 %
Primaries	328.8 %
Shell 5%	541.1 %

4.8 MEDIUM BULK CARRIER, TRANSVERSE FRAMING WITH SPACING 400 MM

The load at which each structural element will reach the permanent deformation limits defined in 3.2.3 are shown in Table 19.

For shell plate and frames, the model behaves in expected way and plastic behavior follows classical plastic hinge mechanism. No instability was observed in framing. As expected, results are close to those of medium LNG tanker and medium dry cargo vessel IA, which have similar scantlings and structural configuration.

For stringer, the model follows classical plastic hinge mechanism. No instability (web buckling or tripping) was observed in the stringer profile before reaching the permanent deformation limit in perpendicular to shell direction. As expected, result is close to that of medium LNG tanker, which has similar scantlings and structural configuration.

For web frames, the behavior was governed by web buckling. This is due to relatively large, unstiffened plate field. Perhaps slightly surprisingly, load at which the webframe buckles is somewhat larger than that of medium LNG tanker, which has similar webframes. These results show that different end supports can have an appreciable effect on the capacity of otherwise similar structure.

Table 19 Loads (as percentage of rule design load) to cause the structural member to reach permanent deformation limit as defined in 3.2.3 for the medium bulk carrier with transverse frames spaced at 400 mm.

Load case	Load
Shell	268.7 %
Frame	280.1 %
Primaries	343.5 %
Shell 5%	395.3 %

4.9 MEDIUM BULK CARRIER, TRANSVERSE FRAMING WITH SPACING 600 MM

The load at which each structural element will reach the permanent deformation limits defined in 3.2.3 are shown in Table 20.

For shell plate and frames, the model behaves in expected way and plastic behavior follows classical plastic hinge mechanism. No instability was observed in framing. Especially for shell plate and slightly also for frame, the capacity is lower than that for vessels with 400 mm and 800 mm frame spacings. This is due to the load formulation in the FSICR, where ice pressure depends on load patch width for patches above 600 mm and is capped at fixed limit for load patches of 600 mm and narrower.

For stringer, the model follows classical plastic hinge mechanism. No instability (web buckling or tripping) was observed in the stringer profile before reaching the permanent deformation limit in perpendicular to shell direction.

For web frames, the behavior was governed by web buckling. This is due to relatively large, unstiffened plate field. Web frame behaves in similar way as other similar vessels in this study.

Table 20 Loads (as percentage of rule design load) to cause the structural member to reach permanent deformation limit as defined in 3.2.3 for the medium bulk carrier with transverse frames spaced at 600 mm..

Load case	Load
Shell	197.5 %
Frame	240.7 %
Primaries	376.7 %
Shell 5%	391.1 %

4.10 MEDIUM BULK CARRIER, TRANSVERSE FRAMING WITH SPACING 800 MM

The load at which each structural element will reach the permanent deformation limits defined in 3.2.3 are shown in Table 21.

For shell plate and frames, the model behaves in expected way and plastic behavior follows classical plastic hinge mechanism. No instability was observed in framing.

For stringer, the model follows classical plastic hinge mechanism. No instability (web buckling or tripping) was observed in the stringer profile before reaching the permanent deformation limit in perpendicular to shell direction.

For web frames, the behavior was governed by web buckling. This is due to relatively large, unstiffened plate field on the webframe web, combined with relatively thin plate of 9 mm. Behavior is similar to other studied vessels.

Table 21 Loads (as percentage of rule design load) to cause the structural member to reach permanent deformation limit as defined in 3.2.3 for the medium bulk carrier with transverse frames spaced at 800 mm.

Load case	Load
Shell	255.4 %
Frame	239.3 %
Primaries	390.8 %
Shell 5%	533.6 %

4.11 MEDIUM BULK CARRIER, LONGITUDINAL FRAMING WITH SPACING 400 MM

The load at which each structural element will reach the permanent deformation limits defined in 3.2.3 are shown in Table 22.

For shell plate and frames, the model behaves in expected way and plastic behavior follows classical plastic hinge mechanism. No instability was observed in framing. Plastic capacity agrees well with that of transversally framed similar vessel.

For web frames, the brackets that connect longitudinal frames to web frames act also as buckling supports for the webframe web. Therefore, unlike with the transversally framed vessel, it was observed that webframe failed first on perpendicular to shell deformation criteria, rather than out-of-plane criteria, on load cases webframe 2 and 3, and capacity for those was higher than for most cases where webframe failed by buckling. For load case webframe 1, buckling failure still governed due to larger web panels at the end brackets. Thus, the capacity of the webframe does not differ much from transverse case.

Table 22 Loads (as percentage of rule design load) to cause the structural member to reach permanent deformation limit as defined in 3.2.3 for the medium bulk carrier with longitudinal frames spaced at 400 mm.

Load case	Load
Shell	309.1 %
Frame	303.5 %
Primaries	423.6 %
Shell 5%	430.7 %

4.12 MEDIUM BULK CARRIER, LONGITUDINAL FRAMING WITH SPACING 600 MM

The load at which each structural element will reach the permanent deformation limits defined in 3.2.3 are shown in Table 23.

For shell plate and frames, the model behaves in expected way and plastic behavior follows classical plastic hinge mechanism. No instability was observed in framing.

For web frames, similarly to longitudinally framed vessel with 400 mm frame spacing, the frame brackets offer buckling support for the webframe web, which is noted as increased load-carrying capacity for load case webframe 2. However, due to larger spacing of 600 mm, the support is less effective, and for loadcase webframe 3, buckling failure lowers the load-carrying capacity significantly, as it becomes the governing loadcase. Overall capacity agrees well with other vessels.

Table 23 Loads (as percentage of rule design load) to cause the structural member to reach permanent deformation limit as defined in 3.2.3 for the medium bulk carrier with longitudinal frames spaced at 600 mm.

Load case	Load
Shell	238.1 %
Frame	376.8 %
Primaries	397.3 %
Shell 5%	561.7 %

4.13 ROPAX

The load at which each structural element will reach the permanent deformation limits defined in 3.2.3 are shown in Table 24.

For shell plate and frames, the model behaves in expected way and plastic behavior follows classical plastic hinge mechanism. No instability was observed in framing.

For stringer, one load case fails with plastic hinge mechanism, while the other fails via web buckling. It can be concluded that this stringer design is just on the border of adequate buckling strength, as the failure mode depends on exact load patch location. The design of the stringer is driven by the ice class requirements, and the resulting capacity aligns well with other vessels.

For web frame, the capacity is limited mainly by web buckling of the webframe, and out-of-plane deformation of the stringer. Similar to stringer, for this vessel the webframe design is driven by the ice class rules.

Table 24 Loads (as percentage of rule design load) to cause the structural member to reach permanent deformation limit as defined in 3.2.3 for the RoPax vessel.

Load case	Load
Shell	243.3 %
Frame	272.5 %
Primaries	403.4 %
Shell 5%	342.0 %

4.14 SUMMARY

All results are summarized in Table 25.

Table 25 Plastic capacity (as percentage of rule design load) to cause the structural member to reach permanent deformation limit as defined in 3.2.3 for all vessels.

Ship	Ice class	Framing		Side	Plastic capacity			
		Direction	Spacing		Shell	Frame	Primaries	Shell 5%
Small dry cargo	IA	T	400	Double	287 %	297 %	473 %	399 %
Medium dry cargo, IC	IC	L	600	Double	363 %	293 %	832 %	732 %
Medium dry cargo, IA	IA	T	400	Double	291 %	277 %	349 %	454 %
Medium dry cargo, IAsuper	IA super	T	400	Double	276 %	321 %	568 %	414 %
Large dry cargo	IA	L	700	Double	311 %	310 %	439 %	557 %
Medium LNG tanker	IA	T	400	Single	270 %	266 %	350 %	403 %
Large tanker	IA	L	800	Double	290 %	287 %	329 %	541 %
Medium bulk carrier, T 400	IA	T	400	Single	269 %	280 %	344 %	395 %
Medium bulk carrier, T 600	IA	T	600	Single	197 %	241 %	377 %	391 %
Medium bulk carrier, T 800	IA	T	800	Single	255 %	239 %	391 %	534 %
Medium bulk carrier, L 400	IA	L	400	Single	309 %	303 %	424 %	431 %
Medium bulk carrier, L 600	IA	L	600	Single	238 %	377 %	397 %	562 %
RoPax	IA super	T	400	Single	243 %	272 %	403 %	342 %
Average					**277 %**	**290 %**	**437 %**	**473 %**
Minimum					**197 %**	**239 %**	**329 %**	**342 %**
Maximum					**363 %**	**377 %**	**832 %**	**732 %**

5 DISCUSSION

5.1 CORRELATION BETWEEN SHIP PARAMETERS AND PLASTIC CAPACITY

Plastic capacity of all vessels is compared in Figure 14 for shell plate and Figure 14 for frames. Average plastic capacity for shell plate is 277 %, and for frames 290 %.

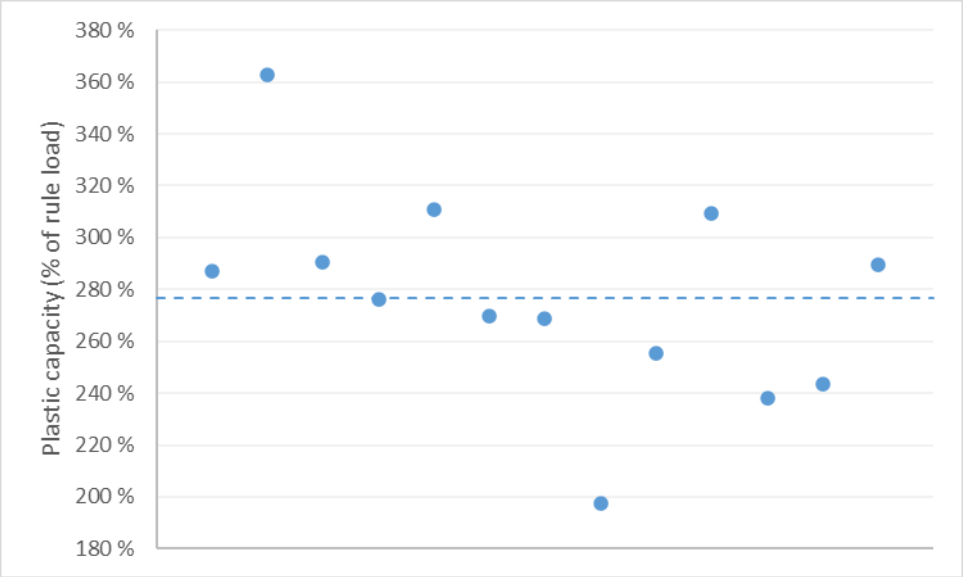

Figure 14 Plastic capacity of shell plating for all vessels (average marked with dashed line).

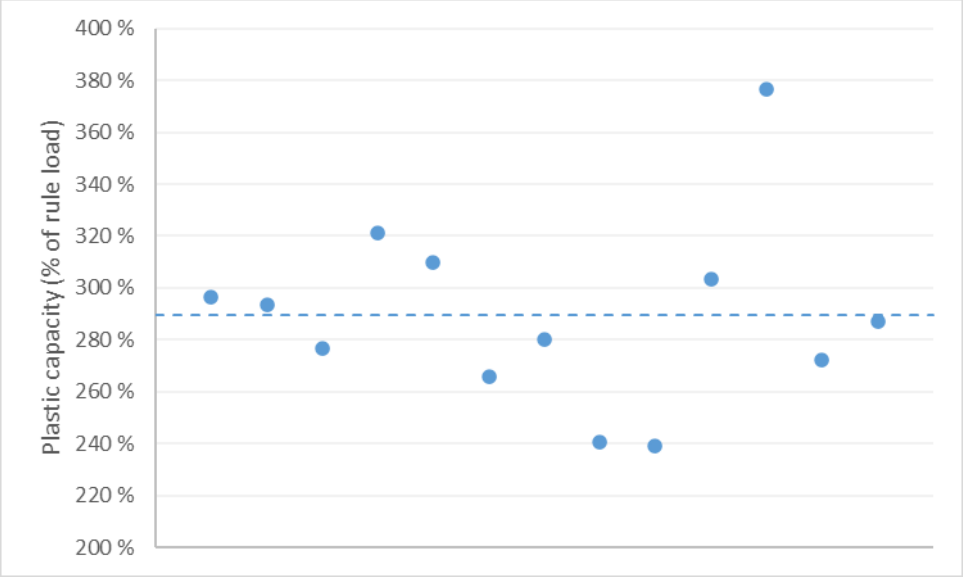

Figure 15 Plastic capacity of frames for all vessels (average marked with dashed line).

The results for primary structures (stringers and web frames) are shown in Figure 16. For some load cases, even though the load was applied on the web frame, the first structure to fail was the stringer, and vice versa. Therefore, the results for these were combined as the primary structures. Medium dry cargo vessels IC and IAsuper have been excluded from the average, as scantlings of these were determined to be clearly driven by other requirements than ice class rules. The average plastic capacity for the primary structures is 386 %. If all vessels with double side construction would be excluded, as it can be questioned if the design for any of these is driven by ice class, the plastic capacity would be 387 %.

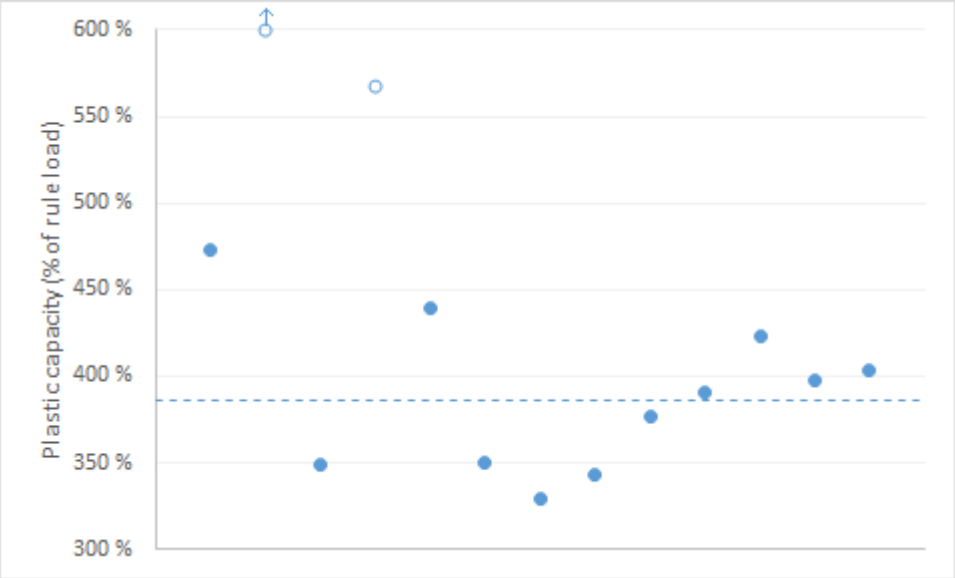

Figure 16 Plastic capacity of primary structures (stringers and web frames) for all vessels. Average marked with dashed line; outliers marked with hollow points are excluded from the average.

Plastic capacity of shell structure up to deformation that represents 5% of frame spacing is shown in Figure 17. In previous HULLFEM project, it was concluded that this represents the upper limit of ice damages on vessels that have been designed to similar strength level as the current rules require. Thus, this can be considered to represent the upper limit of ice loads encountered on the Baltic Sea. The average plastic capacity against permanent deformation of 5 % of frame spacing is 473 % of FSICR design ice load.

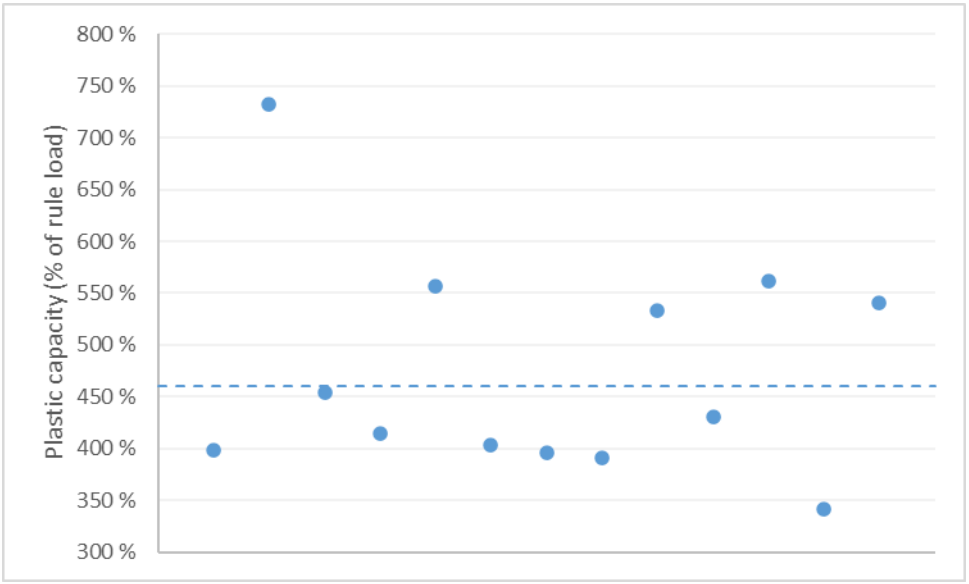

Figure 17 Plastic capacity of shell plating up to 5% of span deformation for all vessels (average marked with dashed line).

On all these plots, some variation between vessels can be observed, as expected. Notable is that there is no clear correlations between capacities of different structural elements, i.e. tendency for the same vessel to have lower or higher capacity on all measures, as shown in Figure 18.

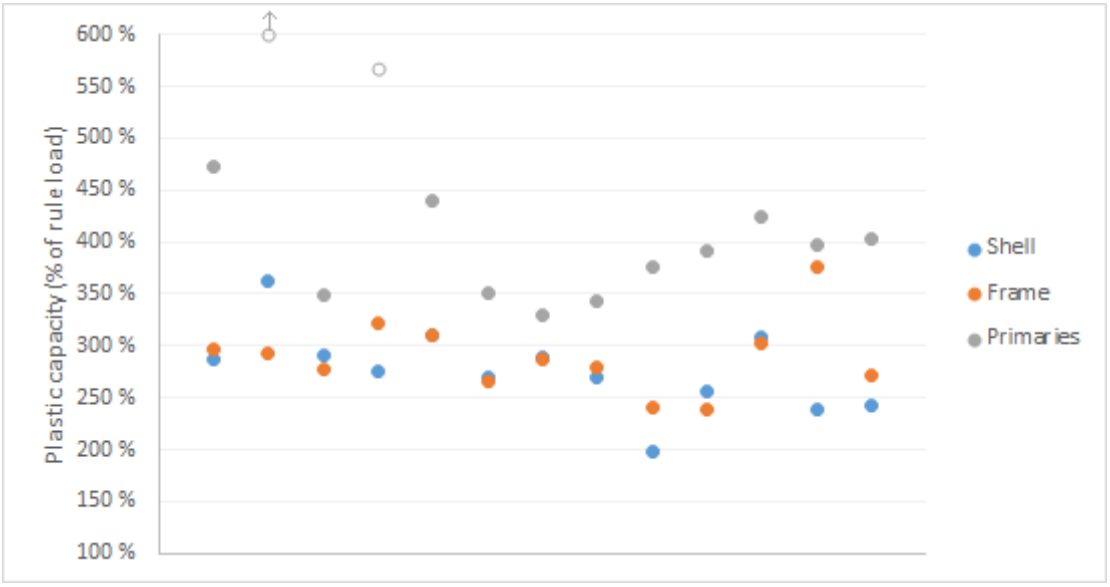

Figure 18 Plastic capacity of shell plate, frames and webframes for all vessels.

Similarly, there seems to be no clear trend so that certain vessel type would have notably higher or lower capacity than others. This can be observed in more detail in Figure 19, which shows that vessel size does not correlate with the plastic capacity. In essence, the results are not dependent on displacement (ship size).

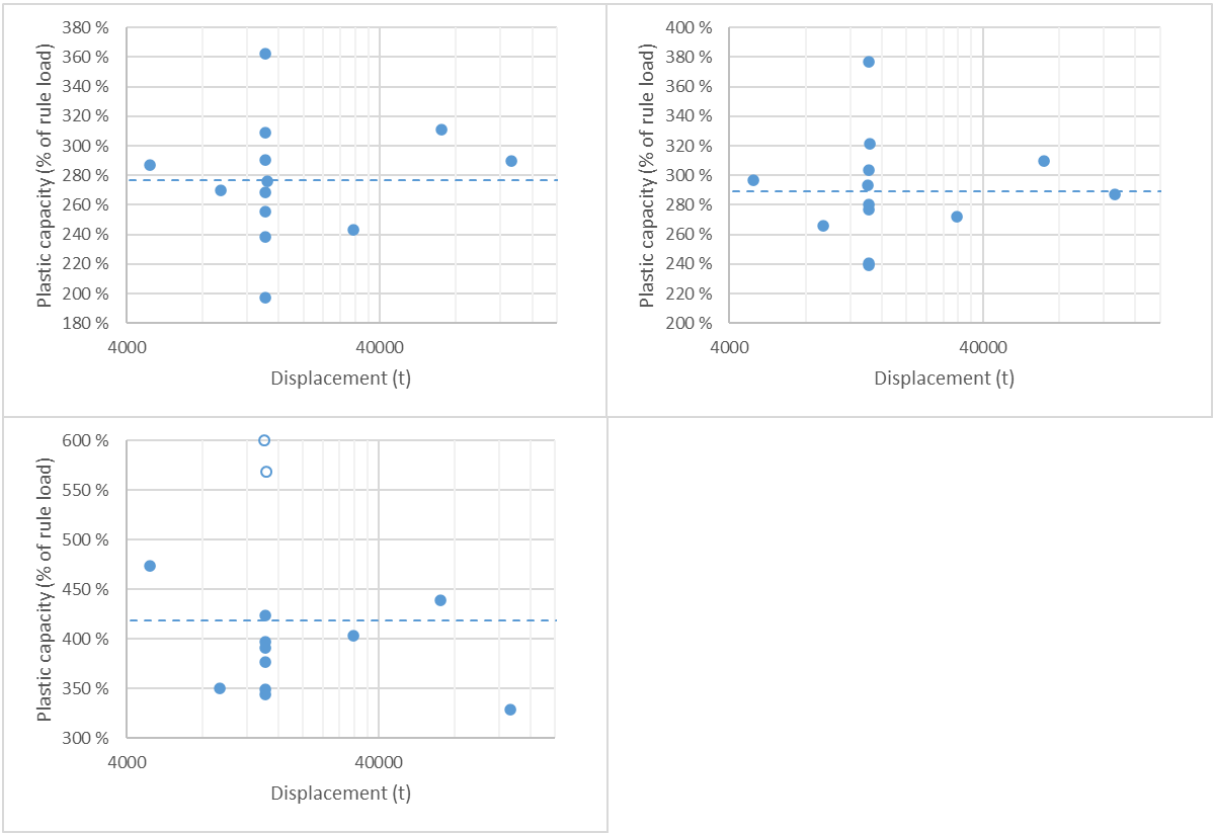

Figure 19 Plastic capacity of shell plate (upper left), frames (upper right) and web frames (lower left) as function of displacement for all vessels.

Correlation between ice class and plastic capacity can be observed in Table 26. It can be seen that there is no correlation between plastic capacity and ice class, i.e. results are not dependent on ice class.

Table 26 Plastic capacity for medium dry cargo vessels with different ice classes.

Ship	Ice class	Framing		Plastic capacity	
		Direction	Spacing	Shell	Frame
Medium dry cargo, IC	IC	L	600	363 %	293 %
Medium dry cargo, IA	IA	T	400	291 %	277 %
Medium dry cargo, IAsuper	IA super	T	400	276 %	321 %

Correlation between framing arrangement and plastic capacity can be observed in Table 27. No clear trends that would lead to higher or lower capacity for certain arrangements can be observed. The only exception is that plastic capacity of vessels with frame spacing of 600 mm are notably lower than those with other spacings. This is result of the chosen load patch width, corresponding to frame spacing, together with the pressure-area relationship in the FSICR, which increases ice pressure with decreasing load area (load patch width), but has a cutoff at 600 mm.

Table 27 Plastic capacity for medium bulk carriers with various framing arrangements.

Ship	Framing		Plastic capacity			
	Direction	Spacing	Shell	Frame	Primaries	Shell 5%
Medium bulk carrier, T 400	T	400	269 %	280 %	344 %	395 %
Medium bulk carrier, T 600	T	600	197 %	241 %	377 %	391 %
Medium bulk carrier, T 800	T	800	255 %	239 %	391 %	534 %
Medium bulk carrier, L 400	L	400	309 %	303 %	424 %	431 %
Medium bulk carrier, L 600	L	600	238 %	377 %	397 %	562 %

Medium dry cargo vessel with ice class IA and medium bulk carrier with transverse framing at 400 mm spacing offer interesting comparison pair. Both vessels are same size, and have similar structural configuration, except that dry cargo vessel has double side with plate-type web frames and stringer platforms, and bulk carrier has single side with open T-beam web frames and stringers.

For stringers and web frames, the capacities are very similar, but limited by different failures, as expected, since the configurations are different. The platforms on double side have significantly higher capacity than the rest of the primaries, due to other requirements than ice class. In double side construction, the capacity is limited by buckling failure of webframe plating between stiffeners. For single side construction, capacity is limited by bending failure of stringer. For both vessels, the results align well with the results of other vessels of this study.

Interestingly, there is a difference in capacity of shell plate, but framing capacity is practically identical. The reason for this difference could not be identified, and the models were checked to be identical in these respects.

Table 28 Plastic capacity for comparable medium dry cargo vessel (with double side) and medium bulk carrier (with single side).

Ship	Plastic capacity			
	Shell	Frame	Primaries	Shell 5%
Medium dry cargo, IA	291 %	277 %	349 %	454 %
Medium bulk carrier, T 400	269 %	280 %	344 %	395 %

Medium LNG tanker and medium bulk carrier with transverse framing and spacing of 400 mm offer another comparison, as both vessels are otherwise similar, but the tanker has a main deck, whereas the bulk carrier has open cross-section. As can be observed in Table 29, the plastic capacities for shell plate and framing are similar, as can be expected. For stringer, the capacities are also similar, and for both, that limits the capacity of the primary structures. The only structural member for which the capacity differs significantly is the web frame, for which the capacity is 381 % for the tanker and 465 % for the bulker. The reason for this is difference in the boundary conditions for the web frame between these vessels, which will affect how the structure behaves and fails.

Table 29 Plastic capacity for medium LNG tanker and medium bulk carrier.

Ship	Plastic capacity			
	Shell	Frame	Primaries	Shell 5%
Small tanker	270 %	266 %	350 %	403 %
Medium bulk carrier, T 400	269 %	280 %	344 %	395 %

Overall, based on the comparisons and observations above, it can be concluded that the proposed method of defining plastic capacity is fairly robust towards variation in vessel size and design, and provides similar measure of capacity regardless of vessel.

5.2 COMPARISON TO HULLFEM I

Plastic capacities for dry cargo vessels, which were first analyzed in previous study [1], were recalculated in this study. The scantlings were modified to be exactly on the rule limits, rather than with typical building practice where plate thicknesses are rounded and stiffener profiles are picked from list of available standard profiles. As can be seen from the results comparison in Table 30, removing these margins has reduced the plastic capacities somewhat, as well as reduced the variation in the results.

In addition, in previous analysis [1] the plastic capacity was determined from the load-displacement curve by assuming that the elastic deformation is proportional to loading using methodology from [8]. For structures that fail with plastic hinge type mechanism, such as shell plate and frames of the studied vessels, this assumption is generally valid with sufficient accuracy. For structures where buckling is the governing failure mode, such as web frames and stringers of the studied vessels, linearity of elastic deformation after onset of buckling is generally not a valid assumption.

For this study, the plastic capacity was determined iteratively, by varying the load and running the analysis until load that results in exactly the set permanent deformation was found. This analysis method removed the assumption of linearity of elastic deformation, which improves accuracy and reliability, especially for buckling-governed problems. As can be seen in Table 30, this has significant effect on the plastic capacity of primary structures.

Table 30 Comparison of plastic capacities for dry cargo vessels calculated in previous and current study.

Shell plate	HULLFEM I	HULLFEM II	Difference
Small dry cargo	362 %	287 %	-21 %
Medium dry cargo, IC	(490 %)	363 %	-
Medium dry cargo, IA	429 %	291 %	-32 %
Medium dry cargo, IAsuper	346 %	276 %	-20 %
Large dry cargo	337 %	311 %	-8 %
Frames	**HULLFEM I**	**HULLFEM II**	**Difference**
Small dry cargo	336 %	297 %	-12 %
Medium dry cargo, IC	390 %	293 %	-25 %
Medium dry cargo, IA	390 %	277 %	-29 %
Medium dry cargo, IAsuper	332 %	321 %	-3 %
Large dry cargo	285 %	310 %	9 %
Primary structures	**HULLFEM I**	**HULLFEM II**	**Difference**
Small dry cargo	472 %	473 %	0 %
Medium dry cargo, IC	1011 %	832 %	-18 %
Medium dry cargo, IA	629 %	349 %	-45 %
Medium dry cargo, IAsuper	543 %	568 %	5 %
Large dry cargo	382 %	439 %	15 %

5.3 PRELIMINARY DESIGN CRITERIA

Based on the results of this study, there is a clear correlation between plastic capacity of structure as defined in 3.2.3 and elastic capacity as defined in the FSICR. As the goal is to end up with similar scantlings, using different criteria for capacity, the design load has to be modified accordingly. For setting the final design load for the new rule proposal, there should be more detailed consideration for design margins etc. As a first, preliminary step, a quick look is made into how the vessels would fare if the rule criteria would be set as the average capacity of all analyzed vessels for each structural element.

Thus, the criteria would be that at 290 % of FSICR design load, the framing should not exceed permanent deformation of 0.3 % of span or 8 mm, whichever is greater. The primary structures should not exceed permanent deformation of 8 mm, at load of 386 % of FSICR design load. If these criteria would be applied to the studied vessels, results would be as shown in Table 31.

Obviously, these results should be viewed with some care, as using the same vessels and analysis set both for developing the criteria and testing it is not rigorous. However, making separate vessel designs and analysis for verification is seen impractical due to high amount of work involved. Thus, it is considered that while this quick analysis is not a proper testing as such, it still provides useful insight into how the proposed rule criteria would work for various vessels.

For most vessels, scantling changes would be within 10 %, which can be considered acceptable, and would not result in major changes in structures compared to typical variation from available profiles, tolerances of plate thicknesses, etc.

For a few cases of framing, slightly greater changes would happen. For transversally framed medium bulk carriers, the framing profile would increase significantly for frame spacings of 600 and 800 mm, most likely due to not quite rigid end support provided by the small open T-beam stringer. For medium bulk carrier with longitudinal framing and spacing of 600 mm, the frame profile could be decreased to be about the same as for 400 mm spacing. This is natural, since both carry the same load patch as the load patch height is less than frame spacing. However, with current FSICR rules, the scantlings still increase for the larger spacing.

For primaries, most vessels would not have significant changes in scantlings. Observing the results of this study, it is likely that most changes would be slight changes of stiffening arrangement, or slight increases in plate thickness to prevent buckling from ice load. These changes would also likely increase the ultimate capacity of the structure and reduce risk of ice damage in case of abnormally high ice load. The vessels which pass the criteria with high margin are the ones where it is likely that the design of the primary structures is mainly driven by other criteria than ice class rules.

Overall, it seems like the proposed criteria would provide a fairly reasonable design basis for these vessels and would generally not result in major changes in the scantlings.

Table 31 Assessment of each vessel against proposed preliminary criteria.

Ship	Frames	Primaries
Small dry cargo	Pass, margin 2 %	Pass, margin 23 %
Medium dry cargo, IC	Pass, margin 1 %	Pass, margin 116 %
Medium dry cargo, IA	Fail, deficit -5 %	Fail, deficit -10 %
Medium dry cargo, IAsuper	Pass, margin 11 %	Pass, margin 47 %
Large dry cargo	Pass, margin 7 %	Pass, margin 14 %
Medium LNG tanker	Fail, deficit -8 %	Fail, deficit -9 %
Large tanker	Fail, deficit -1 %	Pass, margin 5 %
Medium bulk carrier, T 400	Fail, deficit -3 %	Fail, deficit -15 %
Medium bulk carrier, T 600	Fail, deficit -17 %	Fail, deficit -11 %
Medium bulk carrier, T 800	Fail, deficit -17 %	Fail, deficit -2 %
Medium bulk carrier, L 400	Pass, margin 5 %	Pass, margin 1 %
Medium bulk carrier, L 600	Pass, margin 30 %	Pass, margin 10 %
RoPax	Fail, deficit -6 %	Pass, margin 3 %

5.4 RECOMMENDED NEXT STEPS

For the next step, it is recommended that at least one bow is analyzed using similar methodology, to check how shaped hull would affect the results of this study.

In case the results are in line with the results of this study, thought should be given to desired design margins and alignment between current and new design criteria. After that, learnings from this and previous study should be collected and written into a rule proposal. The rule proposal should then be circulated within industry before taking it into use.

6 CONCLUSIONS

Based on the results of this study, it can be concluded that the proportion of the plastic capacity and elastic capacity of structures designed according to current Finnish-Swedish Ice Class Rules is fairly uniform across wide variety of relevant ship types. Moreover, the plastic capacity relative to elastic capacity does not depend appreciably on ship size, ship type, ice class or structural configuration.

Thus, it is possible to formulate design criteria that results in similar scantlings as the current rules but is based on the plastic capacity. To retain equal strength level, design load must be increased when the capacity of the structure is calculated with the proposed plastic limit method. Based on the results of this study, this design load should be approximately 2.77 times the FSICR design load for shell plate, 2.90 times the FSICR design load for frames and 3.86 times the FSICR design load for primary structures. It is emphasized that further consideration of these load levels should be made before writing the rules, and thought should be given to desired margins of safety, alignment with the current rules, etc.

The current study covers the typical vessel types and sizes trading on the Baltic Sea and governed by the FSICR. The current study was done on the parallel midship region, so that several vessel types and sizes could be covered with reasonable analysis effort. Before writing the rule proposal, it is recommended that at least one case of shaped hull region is analyzed to ensure that the proposed method works also for shaped parts of the hull.

After that analysis has been made, and provided that the results align with the results of this study, sufficient basis exists for writing a rule proposal for direct calculation of hull structures for the FSICR.

7 REFERENCES

[1] I. Perälä, K. Katajamäki and V. Valtonen, Direct calculation methods for ice strenghtened hulls in the Finnish-Swedish Ice Class Rules, VTT & Aker Arctic, 30.12.2022.

[2] J. Alanko, Laivan yleissuunnittelu, Turku, 2007.

[3] Traficom, Ice Class Regulations and the Application Thereof, Traficom, 2021.

[4] Dassault Systemes - SIMULIA, Abaqus user's manuals, elements, 2021.

[5] Lloyd's Register, Guidance Notes for Non-Linear Analysis for the Primary Support Structures for Polar Class Vessels, 2022.

[6] DNV, Class guideline CG-0127 Finite element analysis, Ugust 2021.

[7] American Bureau of Shipping, Guidance note on nonlinear finite element analysis of marine and offshore structures, 2021.

[8] V. Valtonen, J. Bond and R. Hindley, "Improved method for non-linear FE analysis of Polar Class ship primary structures," *Marine Structures,* vol. 74, 2020.

[9] International Association of Classification Societies (IACS), Recommendation No.47 Shipbuilding and repair quality standard, IACS, rev. 8, 2017.

[10] P. Kujala, Damage statistics of ice-strengthened ships in the Baltic Sea 1984-1987, Winter Navigation Research Board, Research report No.50.